Design of MKC-442 (Emivirine) Analogues with Improved Activity Against Drug-Resistant HIV Mutants

Andrew L. Hopkins,[†] Jingshan Ren,[†] Hiromichi Tanaka,[‖] Masanori Baba,[§] Mika Okamato,[§] David I. Stuart,[†,‡] and David K. Stammers*,[†]

Laboratory of Molecular Biophysics, Rex Richards Building, South Parks Road, Oxford OX1 3QU, U.K., Oxford Centre for Molecular Sciences, New Chemistry Laboratory, South Parks Road, Oxford OX1 3QT, U.K., Division of Human Retroviruses, Centre for Chronic Viral Diseases, Faculty of Medicine, Kagoshima University, Kagoshima, Japan, and School of Pharmaceutical Sciences, Showa University, Hatanodai 1-5-8, Shinagawa-ku, Tokyo 142, Japan

Received April 20, 1999

Two analogues of the nonnucleoside inhibitor of HIV-1 RT, MKC-442 (emivirine), containing different C6 substituents have been designed to be less susceptible to the commonly found drug-resistance mutation of Tyr181Cys. Compound TNK-6123 had a C6 thiocyclohexyl group designed to have more flexibility in adapting to the mutated drug-binding site. GCA-186 had additional 3′,5′-dimethyl substituents aimed at forming close contacts with the conserved residue Trp229. Both compounds showed ∼30-fold greater inhibitory effect than MKC-442 to the Tyr181Cys mutant virus as well as to the clinically important Lys103Asn virus. X-ray crystallographic structure determination of complexes with HIV-1 RT confirmed the predicted binding modes. These strategies might be used to improve the resilience of other NNRTI series against common drug-resistance mutations.

Introduction

The introduction of multidrug combination therapies has significantly improved the prognosis for patients suffering from HIV-1 infection, leading to a dramatic decline in the death rate from AIDS in the United States and Western Europe.[1,2] However, the administration of multidrug combination therapies, as complicated regimens, can cause difficulties with patient compliance. Noncompliance together with nonideal pharmacokinetics are major factors in the rise of drug resistance. A major challenge facing medicinal chemistry over the next few years will be the development of drugs with significantly improved resistance profiles for chronic use as anti-HIV combination therapy. An important component of such regimens will be nonnucleoside inhibitors of HIV-1 reverse transcriptase (NNRTIs). NNRTIs are a class of structurally diverse aromatic compounds, such as nevirapine, delavirdine, efavirenz, MKC-442 (emivirine), TIBO, and thiocarboxanilides.[3] Structural studies have revealed that NNRTIs inhibit HIV-1 RT by binding to an allosteric site, approximately 10 Å from the polymerase active site,[4−6] causing a distortion of the catalytic aspartate triad.[7] The high selectivity of NNRTIs for HIV-1 RT over HIV-2 RT and cellular polymerases contributes to lower cellular toxicity levels than observed with nucleoside analogues (NRTIs) such as AZT, ddI, or ddC. However this selectivity together with the relatively unconserved amino acid sequence in the drug-binding site has also made most types of NNRTIs susceptible to the rapid selection of drug-resistant virus, particularly when administered as monotherapy either in vitro or in vivo.[8,9] All reported NNRTI-resistant mutations occur in residues surrounding the inhibitor-binding site on the enzyme.[5] A commonly observed drug-resistant virus contains the single amino acid mutation Tyr181Cys.[10] Additionally a Lys103Asn mutation appears relatively frequently in vivo giving resistance to many NNRTIs.[11]

The crystal structures of a range of NNRTIs, including nevirapine, 1051U91, α-APA, HEPT, MKC-442, and TNK-651, complexed with RT[5,12−15] show the importance of the interactions of the aromatic moiety of the inhibitors and the neighboring residues Tyr181, Tyr188, Phe227, and Trp229. The significant contribution of Tyr181 to the binding energy of many NNRTIs is demonstrated by the frequent selection of an escape mutation at this codon, normally with a change to cysteine.[10] The crystal structures have also revealed details of the orientation and geometry of the aromatic interactions between the inhibitors and the surrounding residues. Comparison of the bound conformations of these NNRTIs shows that the orientation of the aromatic groups of many of these inhibitors are conserved within the binding site.[12] An outlier in this analysis is the rather weak binding inhibitor HEPT, which has its phenyl ring rotated by 20−25° due to the loss of interaction with Tyr181.[14] A comparative analysis of complexes of HEPT analogues has suggested structural features that give conformational changes in Tyr181 necessary for tight binding in this series.[14] Kinetic studies of reverse transcriptase that contains the Tyr181Cys mutation show the rate of dissociation of the inhibitor from the enzyme increases relative to wild type.[16]

Results and Discussion

Modifications to MKC-442 (Emivirine) in the C6 Position. In this work we investigate modifications to the group interacting with Tyr181 in order to minimize the loss of binding energy in the presence of the Tyr181Cys mutation. We have investigated two approaches. First the replacement of the benzyl moiety

[†] Rex Richards Building.
[‡] New Chemistry Laboratory.
[§] Kagoshima University.
[‖] Showa University.

10.1021/jm990192c CCC: $18.00
Published on Web 10/09/1999

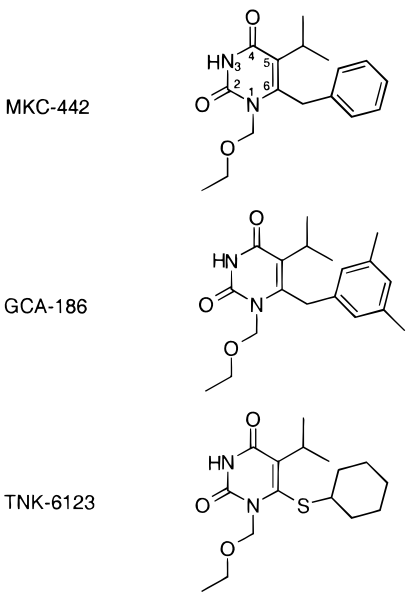

Figure 1. Chemical structures of MKC-442, GCA-186, and TNK-6123. The 6 position substituents (benzyl, 3′,5′-dimethylbenzyl, and thiocyclohexyl of MKC-442, GCA-186, and TNK-6123, respectively) were chosen to observe their effects on the inhibition of wild type and resistant strains of HIV-1 RT.

by a thiocyclohexyl group [TNK-6123 (6-cyclohexylthio-1-ethoxymethyl-5-isopropyluracil)] (Figure 1). We reasoned that since the cyclohexyl moiety has greater conformational flexibility than a planar aromatic ring, it could adapt to a mutated drug pocket and the thioether linkage should allow a closer fit within the hydrophobic subpocket. Second introduction of *m*-dimethyl substituents onto the phenyl ring [GCA-186 (6-(3′,5′-dimethylbenzyl)-1-ethoxymethyl-5-isopropyluracil)] intended to optimize interactions with Trp229, thereby reducing the dependence on binding to Tyr181. Molecular modeling suggests that methyl groups attached to the 3 and 5 positions of the 6-benzyl group of MKC-442 would sit comfortably in a deep hydrophobic region beneath Trp229. Trp229 is highly conserved in immunodeficiency virus reverse transcriptases, suggesting that an important functional role for this residue renders it less mutable.

Antiviral Activity of MKC-442 Analogues. The inhibition effects of the compounds MKC-442, GCA-186, and TNK-6123 on the replication of HIV-1 were examined. The compounds were tested for antiviral activity against wild-type and two drug-resistant strains of HIV-1. The two drug-resistant strains contained single amino acid changes: Tyr181Cys and Lys103Asn, respectively. The results of the antiviral inhibition assays are shown in Table 1. Either amino acid change, within the NNRTI binding site of reverse transcriptase, is sufficient to reduce sensitivity to MKC-442 by over 3 log units. Interestingly the antiviral results show that both of the analogues with C6 modifications have significantly improved inhibition of the Tyr181Cys mutant as planned. The Tyr181Cys mutation provides a 3000-fold reduced sensitivity to MKC-442, but TNK-6123 and GCA-186 are only 90- and 134-fold less potent toward this mutant, respectively. Additionally, and surprisingly, the activity was also significantly improved against the Lys103Asn mutant over their parent compound. The Lys103Asn mutation provides over a 1000-fold resistance to MKC-442, while GCA-186 shows only a 37-fold decrease in potency (EC_{50} = 40 nM) and TNK-6123 shows a slightly greater loss of potency (78-fold). The EC_{50} values for GCA-186 and TNK-6123 against both mutants are well below 300 nM. Interestingly, TNK-6123 shows a nearly consistent decrease of potency against both the Tyr181Cys and Lys103Asn mutants, of about 80-fold.

Table 1. Inhibition Effect of MKC-442 Analogues on Replication of HIV-1

	EC_{50} (μM) for HIV-1 strain[a]				CC_{50}
compd	III_B	$III_{B-R(Y181C)}$	NL4-3	NL4-3_{K103N}	(μM)[b]
MKC-442	0.004	13.4	0.001	1.26	>100
GCA-186	0.001	0.18	0.001	0.04	52.5
TNK-6123	0.003	0.27	0.003	0.25	74.8

[a] Based on the inhibition of HIV-1-induced focus formation in MAGI-CCR5 cells. [b] Based on the reduction of viability of mock-infected cells. Data quoted are the means of two independent experiments.

Crystal Structures of GCA-186 and TNK-6123 Complexed with RT. To test whether the new analogues bind to HIV-1 RT as predicted, the crystal structures of RT−TNK-6123 and RT−GCA-186 complexes were determined. Electron density maps for each of the complexes reveal GCA-186 and the TNK-6123 bound at the NNRTI site (Figure 2). The orientation and position of GCA-186 and TNK-6123 are broadly similar to our previously reported complex with MKC-442.[14] Differences between the MKC-442, GCA-186, and TNK-6123 complexes are found in the conformation of these inhibitors, the water structure in the NNRTI site, and contacts between the inhibitors and the protein (Figure 3).

In common with previously determined HEPT analogues in complexes with RT, the pyrimidine rings of GCA-186 and TNK-6123 are orientated by a hydrogen bond from N3 to the main chain carbonyl oxygen of Lys101, pinning the ring between Leu100 and Val106. The 1-ethoxymethyl substituents of both GCA-186 and TNK-6123 adopt conformations similar to that found for this substituent in the MKC-442 complex. Consequently the flexible Pro236 loop, which tracks the 1-ethoxymethyl groups, occupies the same position in all three complexes. The 5-isopropyl substituents of GCA-186 and TNK-6123 occupy the subpocket below Tyr181 and adopt the same rotamer conformation observed for MKC-442.

Each of the three inhibitors is also orientated by a water molecule which forms a trio of hydrogen bonds to the C4 carbonyl oxygen of the pyrimidine ring of the inhibitor, the main chain nitrogen of Lys101, and a side chain carboxy oxygen of Glu138(p51) (Figure 4). A second well-ordered water molecule forms a hydrogen bond to the main chain Lys103 carbonyl oxygen and makes van der Waals contacts with the 1-ethoxymethyl substituent in the MKC-442, GCA-186, and TNK-6123 complexes. In the RT−GCA-186 and RT−MKC-442 complexes, there is weak density for a third water molecule, which forms four bonds, in a tetrahedral arrangement between the C2 carbonyl oxygen of the inhibitor, the main chain nitrogen of residue Lys103, the carbonyl oxygen of Pro236, and the water molecule which H-bonds to the carbonyl oxygen of Lys103. A larger C2 substituent may be able to occupy the space

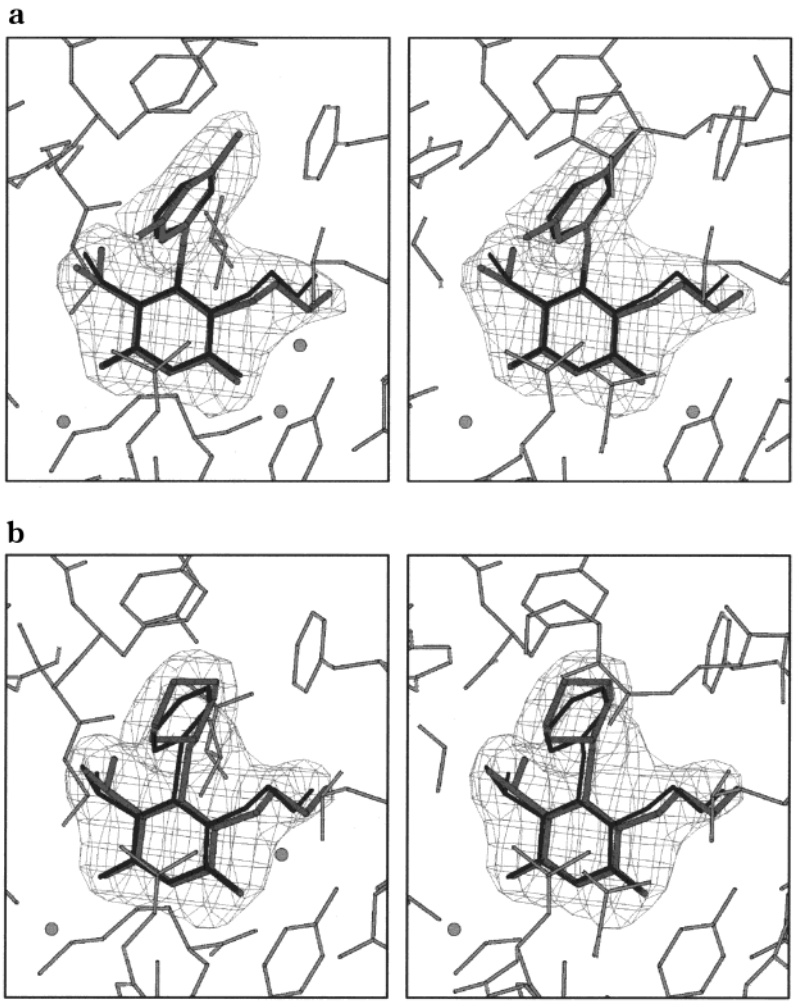

Figure 2. Stereodiagrams of simulated annealing omit electron density maps for (a) GCA-186 and (b) TNK-6123 bound to HIV-1 RT. The maps are contoured at 3σ. The inhibitors (thicker bonds) and the protein (thinner bonds) are shown in gray. In each case MKC-442 is also superimposed and shown in black. Water molecules are represented as gray spheres.

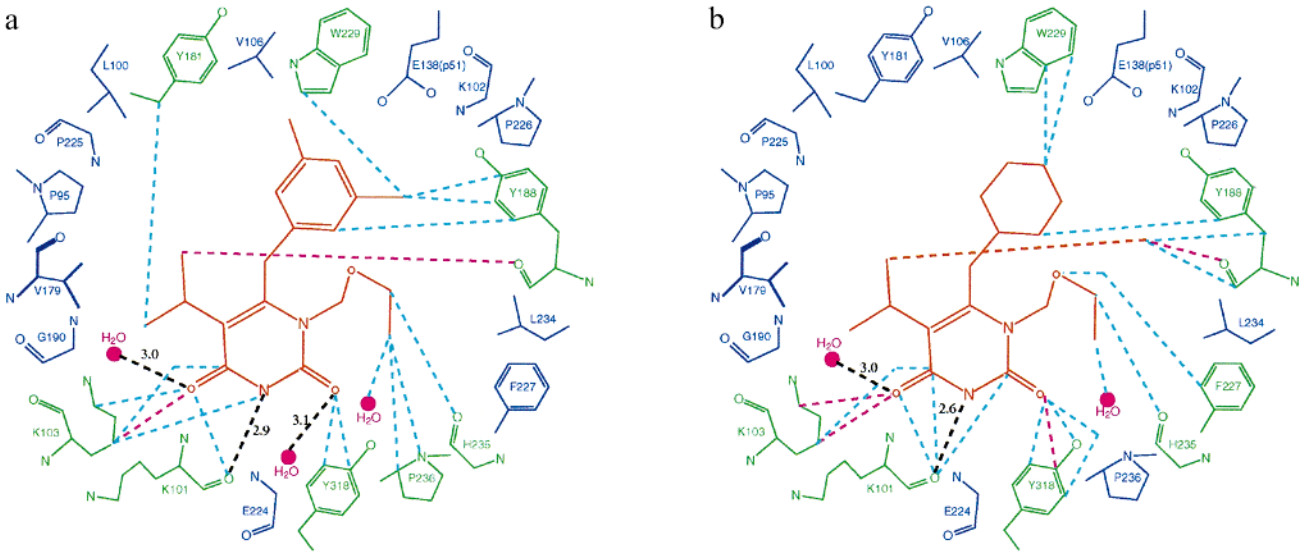

Figure 3. Schematic diagram showing the intermolecular interactions between the NNRTIs (in red) and the surrounding residues of HIV-1 RT for (a) GCA-186 and (b) TNK-6123. The pink spheres represent water molecules in contact with the inhibitor. Residues which contact the NNRTI with a minimum interatomic distance of <3.6 Å are shown in green, while other residues lining the binding pocket are shown in blue. The individual distances between the NNRTI and the protein atoms are shown as dashed lines (d <= 3.3 Å in pink; 3.3 < d <= 3.6 Å in light blue; potential hydrogen bonds are shown with distances in black).

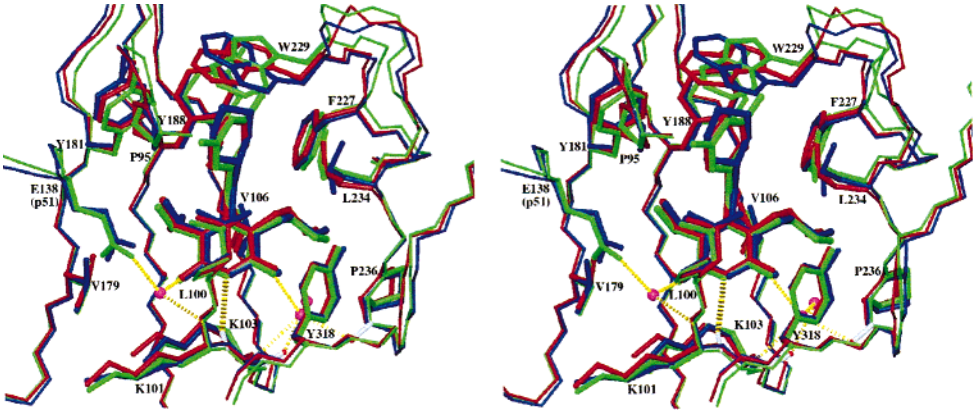

Figure 4. Stereodiagram showing the superimposition of GCA-186 (in green), TNK-6123 (in blue), and MKC-442 (in red) in their binding sites on HIV-1 RT. The inhibitors and protein side chains are shown as thicker ball-and-stick representations and the protein main chain backbone as thinner lines. For clarity, only water molecules (magenta spheres) in the NNRTI site of the RT−GCA-186 complex together with hydrogen bonds (yellow broken sticks) to these waters and GCA-186 are shown. The structures were superimposed using the method described previously.[5]

of these two water molecules, thereby enabling the inhibitor to form hydrogen bonds to the main chain nitrogen of residue Lys103 (in an analogous way to BHAP[15]). This type of interaction is obviously less susceptible to disruption by side chain mutation.

Interactions with C6 Substituents. The important difference in the chemical structures between MKC-442, GCA-186, and TNK-6123 is the nature of the pyrimidine C6 substituents. The C6 substituents are positioned in the upper subpocket of the NNRTI binding site, which is formed between Leu100, Tyr181, Tyr188, Phe227, and Trp229. The 6-cyclohexylthio substituent of TNK-6123 fills the upper subpocket of the NNRTI binding site, adopting the lowest-energy 'chair' conformation. The longer carbon−sulfur bonds of the thioether linker allow the cyclohexyl group to sit deeper within the upper subpocket. The cyclohexyl ring of TNK-6123 is puckered, and yet the plane of the ring overall matches the 6-benzyl ring of MKC-442. Although GCA-186 shows far greater potency against both the Tyr181Cys- and Lys103Asn-resistant HIV-1 strains, the 6-(3,5-dimethylbenzyl) group has a similar conformation to the corresponding 6-benzyl group of MKC-442. The relative conformations for the rings of the C6 substituents for the three inhibitors, bound at the NNRTI pocket, as defined by the dihedral angles N1−C6−X−C1 (ω_1) and C6−X−C1′−C2′ (ω_2) are: $\omega_1 = -78°$, $\omega_2 = 142°$ for MKC-442 (X = CH_2), $\omega_1 = -73°$, $\omega_2 = 164°$ for TNK-6123 (X = S), and $\omega_1 = -77°$, $\omega_2 = 148°$ for GCA-186 (X = CH_2), respectively. The most important features of the binding of GCA-186 compared to MKC-442 are contacts to the protein made by the additional 3,5-di-*m*-methyl groups of the 6-benzyl ring. These occupy previously unexploited hydrophobic space near the 'roof' of the NNRTI binding pocket and make numerous weak van der Waals contacts (4.0 Å or less) to residues Pro95, Leu100, Tyr181, Tyr188, Phe227, Trp229, and Leu234 (Figure 3). Due to the close packing of the hydrophobic residues, the extra *m*-methyls fit comfortably into the space available and exploit extra van der Waals contacts. The addition of the two *m*-methyls increases the surface area of the drug shielding the perpendicular plane of Trp229 by 20 $Å^2$, compared to MKC-442.

The conformational heterogeneity of Trp229 that we previously noted[13] is reflected in the observation that for the GCA-186 and MKC-442 complexes the side chain adopts two conformations, whereas the TNK-6123 complex selects a single conformer.

Structural Basis for Inhibition of Mutant HIV. The results presented above show that modification of the C6 substituent, 6-benzyl of MKC-442, to either 6-thiocyclohexyl (TNK-6123) or 6-(3′,5′-dimethylbenzyl) (GCA-186) results in the partial rescue of the inhibitors from the effects of the two most common single-point resistance mutations seen for NNRTIs, Tyr181Cys and Lys103Asn. The crystal structures of the GCA-186 and TNK-6123 complexes show that the binding modes of analogues are in line with predictions. The 6-thiocyclohexyl is a direct spatial replacement for 6-benzyl, but with slightly greater hydrophobic character. The 6-thio linker of TNK-6123 places the cyclohexyl ring slightly deeper into 'upper' hydrophobic region of the NNRTI pocket. The similarity between the structures of the RT−GCA-186 and RT−MKC-442 complexes indicates the significant differences in behavior against the drug-resistant mutants is fully explained by the presence of the additional *m*-methyl groups, buried in a deep hydrophobic region of the NNRTI binding site, considerably increasing the van der Waals contacts to the conserved Trp229 (Figure 3).

We believe that TNK-6123 retains activity against the Tyr181Cys mutant partly because of the greater flexibility of the cyclohexyl substituent, which allows it to better adapt to the mutated drug-binding pocket. An additional factor that could contribute to TNK-6123 binding tightly to Tyr181Cys when compared to MKC-442 is the reduction of unfavorable $\pi-\pi$ stacking with the side chain of Tyr188 on the replacement of the benzyl group with thiocyclohexyl. The electronic nature of the $\pi-\pi$ interactions favors the stacking of aromatic rings either by parallel-displaced (off-center) or edge-on (T-stacking) geometries, while the face-to-face geometry is unfavorable (particularly in environments where there is a low effective dielectric constant), since the dominant interaction is π-electron repulsion.[17,18] The unfavorable face-to-face stacking observed between MKC-442 and Tyr188 would be eliminated by the substitution of the nonaromatic cyclohexyl group of TNK-6123. In the mutated RT containing Tyr181Cys, the nonaromatic cyclohexyl group of TNK-6123 is not

restricted by $\pi-\pi$ stacking geometry and therefore free to optimize van der Waals contacts.

In the case of GCA-186, the addition of the *m*-methyl interactions results in the burying of an extra 60 Å^2 of accessible surface area compared to MKC-442, in a highly hydrophobic region of the NNRTI binding site. The additional interactions observed in the GCA-186 complex with the side chain of the conserved Trp229, as well as other residues in this region, result in the compound deriving a smaller fraction of its binding energy from the interaction with the Tyr181 side chain.

The unexpected observation that both TNK-6123 and GCA-186 have significantly improved activity against the clinically important Lys103Asn mutant RT when compared to the parent compound MKC-442 is an important finding, since this greatly increases their potential as drug candidates. However it is not obvious what the structural basis for this improved binding to Asn103 may be. Since both GCA-186 and TNK-6123 have greater bulk distal to the pyrimidine ring (the closest part of the inhibitors to the Asn103), an indirect mechanism is likely. This could relate to an improved presentation of the pyrimidine ring to make a hydrogen bond to the mutated side chain of Asn103.

Conclusions

We believe that strategies we have described, to improve the activity of NNRTIs against drug-resistant RT mutants, could have general utility for the design of NNRTIs with markedly improved resistance profiles. A combination of both of these strategies might lead to an even greater inhibition of these two common HIV mutants.

Experimental Section

Synthetic Chemistry. The preparation of GCA-186 has been reported.[19] TNK-6123 (6-cyclohexylthio-1-ethoxymethyl-5-isopropyluracil) was synthesized as follows: To a THF (10 mL) solution of lithium 2,2,6,6-tetramethylpiperidide (3.2 mmol) was added 1-ethoxymethyl-5-isopropyluracil (309 mg, 1.46 mmol) in THF (8 mL) dropwise while maintaining the temperature below −70 °C. Dicyclohexyl disulfide (740 μL, 3.37 mmol) was then added to this solution. The reaction mixture was stirred for 4 h at below −70 °C and was then quenched with AcOH, evaporated, and partitioned between $CHCl_3$ and saturated $NaHCO_3$. Silica gel chromatography ($CHCl_3$) of the organic layer gave TNK-6123 (136 mg, 29%) as a syrup. An analytically pure solid sample (mp 97−98 °C) was obtained by HPLC (hexane/EtOAc = 4:1) purification: ^{1}H NMR ($CDCl_3$, 500 MHz) δ 1.19 (3H, t, OCH_2*Me*), 1.29 (6H, d, CH*Me*$_2$), 1.21−1.34 (3H, m, cyclohexyl), 1.36−1.43 (2H, m, cyclohexyl), 1.60−1.63 (1H, m, cyclohexyl), 1.76−1.80 (2H, m, cyclohexyl), 3.24 (1H, m, cyclohexyl), 3.55 (1H, m, C*H*Me$_2$), 3.63 (2H, q, O*CH*$_2$-Me), 5.61 (2H, s, NCH_2O), 9.33 (1H, br, NH); FAB-MS *m*/*z* 327 ($M^+ + H$). Anal. Calcd for $C_{16}H_{26}N_2O_3S$: C, 58.87; H, 8.03; N, 8.58. Found: C, 59.05; H, 8.16; N, 8.57.

Antiviral Assay. The antiviral effects of the compounds on HIV-1 replication were determined by monitoring the inhibition of virus-induced cytopathicity in MAGI-CCR5 cells,[20] which are susceptible to both macrophage-tropic and T-cell line-adapted HIV-1 strains. The cells were propagated in DMEM supplemented with 10% fetal bovine serum (FBS), 100 U/mL penicillin G, 0.1 mg/mL streptomycin, 0.2 mg/mL G418, 0.1 mg/mL hygromycin B, and 1 μg/mL puromycin. The III_B strain of HIV-1, its Tyr181Cys mutant (III_{B-R}),[21] the molecular clone NL4-3, and its mutant NL4-3$_{k103N+}$ were used in the anti HIV-1 assays. The virus strains were propagated in MT4 cells. The titers of virus stocks were stored at −80 °C prior to use.

To determine the activities of the compounds, the cells (1×10^4 cells/well) were cultured in a microtiter plate and incubated for 24 h. The culture medium was then removed, infected with HIV-1 (approximately 300 focus-inducing units/well), and incubated in the presence of various concentrations of the test compounds. DMEM supplemented with only FBS, penicillin G, and streptomycin was used in the assay. After a 2-day incubation at 37 °C, the cells were fixed with 1% formaldehyde and 0.2% glutaraldehyde in PBS for 5 min and washed twice with PBS. The cells were treated with staining solution containing X-Gal at 37 °C for 50 min and washed with PBS. The number of staining cells was determined microscopically. The cytotoxicities of the compounds were evaluated in parallel with their antiviral activities. The evaluation was based on the viability of mock-infected cells, as monitored by the MTT method.[22]

Table 2. Crystallographic Statistics for RT−GCA-186 and RT−TNK-6123 Complexes

complex	RT−GCA-186	RT−TNK-6123
data collection details:		
data collection site	BL6A2, PF	7.2, SRS
temperature (K)	289	100
wavelength (Å)	1.0	1.488
collimation (mm)	0.1	0.2
number of crystals	2	1
unit cell (Å)	140.0, 111.5, 73.2	136.8, 109.5, 71.7
crystal form	C	E
data processing details:		
resolution range (Å)	20.0−2.5	30.0−2.5
observations	179492	99833
unique reflections	37000	35239
completeness (%)	91.8	92.7
reflections with $F/\sigma(F) > 3$	26588	26281
R_{merge} (%)[a]	15.3	10.4
outer resolution shell:		
resolution range (Å)	2.6−2.5	2.6−2.5
unique reflections	3034	3319
completeness (%)	68.4	80.0
reflections with $F/\sigma(F) > 3$	752	1202
refinement statistics:		
resolution range (Å)	20.0−2.5	30.0−2.5
unique reflections	37000	35239
R-factor[b] *R*-working/*R*-free	0.198/0.255	0.232/0.315
protein atoms	7808	7832
inhibitor atoms	24	22
water molecules	56	142
rms bond length deviation (Å)	0.007	0.007
rms bond angle deviation (deg)	1.3	1.4
mean *B*-factor (Å^2)[c]	52/58/47/30	45/50/32/24
B-factor deviation (Å^2)[d]	4.0	3.4

[a] $R_{merge} = \Sigma|I - \langle I\rangle|/\Sigma\langle I\rangle$ [b] *R*-factor $= \Sigma||F_{obs}| - |F_{calc}||/\Sigma|F_{obs}|$. [c] Mean *B*-factor for main chain, side chain, water, and inhibitor atoms, respectively. [d] rms deviation between *B*-factors for bonded main chain atoms. For the RT−GCA-186 complex, residues 89−90 and 544−560 in the p66 subunit and residues 1−4, 89−92, 218−230, and 436−440 in the p51 subunit were missing from the electron density and were omitted from the model. For the RT−TNK-6123 complex, residues 540−560 from the p66 subunit and residues 89−92 and 216−231 from the p51 subunit are not included in the protein model since the electron density for these stretches of sequence was ill-defined.

Crystallization and Data Collection. Crystals (space group $P2_12_12_1$) of the RT−GCA-186 and RT−TNK-6123 complexes were grown and equilibrated in 50% PEG 3350 following the previously reported protocols.[23] The RT−GCA-186 and RT−TNK-6123 crystals belong to crystal forms C and E, respectively.[24]

X-ray diffraction data for the RT−GCA-186 complex were collected at 289 K, from two crystals with synchrotron radiation at the Photon Factory, KEK, using the Weissenberg method, image plate system and other experimental procedures as described previously.[5] 3.5° oscillations and a coupling constant of 1.5°/mm with an exposure time of 120 s and 5° skip between images were used.

Diffraction data for the RT−TNK-6123 complex were collected at 100 K, at the SRS, Daresbury Laboratory, U.K., using the oscillation method with a 30-cm MAR imaging plate in 18-cm diameter mode.

Data processing was with the DENZO and SCALEPACK packages.[25] Data sets >90% complete to 2.5 Å resolution were obtained for both complexes. Crystallographic statistics are presented in Table 2.

Structure Determination and Refinement. The structures were solved by molecular replacement using procedures described previously.[12] RT−1051U91 coordinates (1RTH)[5] were used for the RT−GCA-186 dataset, and the RT−TNK-6123 dataset was solved using the protein model of the RT−MKC-442 complex (1RT1).[14] The RT−GCA-186 and RT−TNK-6123 datasets were sharpened using overall anisotropic *B* factor scaling. All refinement protocols were performed using X-PLOR[26] or CNS.[27] Difference ($|F_{obs}| - |F_{calc}|$) maps allowed the unambiguous positioning and orientation of inhibitors bound at the nonnucleoside inhibitor binding site. The models were rebuilt using the program FRODO[28] on an ESV workstation. Crystallographic statistics for the structure determinations are given in Table 2. Diagrams of structures were prepared using BOBSCRIPT[29] and rendered with RASTER-3D.[30]

The coordinates and structure factors for the RT−GCA-186 and RT−TNK-6123 complexes have been deposited with the Protein Data Bank and are scheduled for release 1 year after publication (PDB ID Codes 1c1b and 1c1c, respectively).

Acknowledgment. We thank the UK MRC for long-term funding of the RT work with grants to D.K.S. and D.I.S. D.I.S. is a member of the TARA project. Part of this study was supported by the Grant-in-Aid for Scientific Research (c) (No. 09672159) to H.T., from the Ministry of Education, Science, Sports and Culture, Japan. The MAGI-CCR5 cells were obtained from the AIDS Research and Reference Reagent Program, National Institute of Allergy and Infectious Diseases, Bethesda, MD (contributor, J. Overbauch).

References

(1) rettle, R. P.; Wilson, A.; Povey, S.; Morris, S.; Morgan, R.; Leen, C. L.; Hutchinson, S.; Lewis, S.; Gore, S. Combination therapy for HIV: the effect on inpatient activity, morbidity and mortality of a cohort of patients. *Int. J. STD. AIDS* **1998**, *9*, 80−87.

(2) Mocroft, A.; Vella, S.; Benfield, T. L.; Chiesi, A.; Miller, V.; Gargalianos, P.; d'Arminio-Monforte, A.; Yust, I.; Bruun, J. N.; Phillips, A. N.; Lundgren, J. D. Changing patterns of mortality across Europe in patients infected with HIV-1. EuroSIDA Study Group. *Lancet* **1998**, *352*, 1725−1730.

(3) De Clercq, E. The role of nonnucleoside reverse transcriptase inhibitors (NNRTIs) in the therapy of HIV-1 infection. *Antiviral Res.* **1998**, *38*, 153−179.

(4) Kohlstaedt, L. A.; Wang, J.; Friedman, J. M.; Rice, P. A.; Steitz, T. A. Crystal structure at 3.5 Å resolution of HIV-1 reverse transcriptase complexed with an inhibitor. *Science* **1992**, 256, 1783−1790.

(5) Ren, J.; Esnouf, R.; Garman, E.; Somers, D.; Ross, C.; Kirby, I.; Keeling, J.; Darby, G.; Jones, Y.; Stuart, D.; Stammers, D. High-resolution structures of HIV-1 RT from four RT-inhibitor complexes. *Nature Struct. Biol.* **1995**, *2*, 293−302.

(6) Ding, J.; Das, K.; Tantillo, C.; Zhang, W.; Clark, A. D. J.; Jessen, S.; Lu, X.; Hsiou, Y.; Jacobo-Molina, A.; Andries, K.; Pauwels, R.; Moereels, H.; Koymans, L.; Janssen, P. A. J.; Smith, R. H. J.; Kroeger Koepke, R.; Michejda, C. J.; Hughes, S. H.; Arnold, E. Structure of HIV-1 reverse transcriptase in a complex with the nonnucleoside inhibitor α-APA R 95845 at 2.8 Å resolution. *Structure* **1995**, *3*, 365−379.

(7) Esnouf, R.; Ren, J.; Ross, C.; Jones, Y.; Stammers, D.; Stuart, D. Mechanism of inhibition of HIV-1 reverse transcriptase by nonnucleoside inhibitors. *Nature Struct. Biol.* **1995**, *2*, 303−308.

(8) Richman, D.; Shih, C.-K.; Lowy, I.; Rose, J.; Prodanovich, P.; Goff, S.; Griffin, J. Human immunodeficiency virus type 1 mutants resistant to nonnucleoside inhibitors of reverse transcriptase arise in tissue culture. *Proc. Natl. Acad. Sci. U.S.A.* **1991**, *88*, 11241−11245.

(9) Richman, D. D.; Havlir, D.; Corbeil, J.; Looney, D.; Ignacio, C.; Spector, S. A.; Sullivan, J.; Cheeseman, S.; Barringer, K.; Pauletti, D.; Shih, C.-K.; Myers, M.; Griffin, J. Nevirapine resistance mutations of human immunodeficiency virus type 1 selected during therapy. *J. Virol.* **1994**, *68*, 1660−1666.

(10) Larder, B. A. Interactions between drug resistance mutations in human immunodeficiency virus type 1 reverse transcriptase. *J. Gen. Virol.* **1994**, *75*, 951−957.

(11) Schinazi, R. F.; Larder, B. A.; Mellors, J. W. Mutations in retroviral genes associated with drug resistance. *Int. Antiviral News* **1997**, *5*, 129−135.

(12) Ren, J.; Esnouf, R.; Hopkins, A.; Ross, C.; Jones, Y.; Stammers, D.; Stuart, D. The structure of HIV-1 reverse transcriptase complexed with 9-chloro-TIBO: lessons for inhibitor design. *Structure* **1995**, *3*, 915−926.

(13) Ren, J.; Esnouf, R. M.; Hopkins, A. L.; Warren, J.; Balzarini, J.; Stuart, D. I.; Stammers, D. K. Crystal structures of HIV-1 reverse transcriptase in complex with carboxanilide derivatives. *Biochemistry* **1998**, *37*, 14394−14403.

(14) Hopkins, A. L.; Ren, J.; Esnouf, R. M.; Willcox, B. E.; Jones, E. Y.; Ross, C.; Miyasaka, T.; Walker, R. T.; Tanaka, H.; Stammers, D. K.; Stuart, D. I. Complexes of HIV-1 reverse transcriptase with inhibitors of the HEPT series reveal conformational changes relevant to the design of potent nonnucleoside inhibitors. *J. Med. Chem.* **1996**, *39*, 1589−1600.

(15) Esnouf, R. M.; Ren, J.; Hopkins, A. L.; Ross, C. K.; Jones, E. Y.; Stammers, D. K.; Stuart, D. I. Unique features in the structure of the complex between HIV-1 reverse transcriptase and the bis-(heteroaryl)piperazine (BHAP) U-90152 explain resistance mutations for this nonnucleoside inhibitor. *Proc. Natl. Acad. Sci. U.S.A.* **1997**, *94*, 3984−3989.

(16) Maga, G.; Amacker, M.; Ruel, N.; Hubscher, U.; Spadari, S. Resistance to nevirapine of HIV-1 reverse transcriptase mutants: loss of stabilizing interactions and thermodynamic or steric barriers are induced by different single amino acid substitutions. *J. Mol. Biol.* **1997**, *274*, 738−747.

(17) Hunter, C. A.; Sanders, J. K. M. The nature of $\pi-\pi$ interactions. *J. Am. Chem. Soc.* **1990**, *112*, 5525−5534.

(18) McGaughey, G. B.; Gagnes, M.; Rappe, A. K. π-stacking interactions. *J. Biol. Chem.* **1998**, *273*, 15458−15463.

(19) Tanaka, H.; Takashima, H.; Ubasawa, M.; Sekiya, K.; Inouye, N.; Baba, M.; Shigeta, S.; Walker, R. T.; De Clercq, E.; Miyasaka, T. Synthesis and antiviral activity of 6-benzyl analogues of 1-[(2-hydroxyethoxy)methyl]-6-(phenylthio)thymine (HEPT) as potent and selective anti-HIV-1 agents. *J. Med. Chem.* **1995**, *38*, 2860−2865.

(20) Chackerian, B.; Long, E. M.; Luciw, P. A.; Overbaugh, J. Human immunodeficiency virus type 1 coreceptors participate in postentry stages in the virus replication cycle and function in simian immunodeficiency virus infection. *J. Virol.* **1997**, *71*, 3932−3939.

(21) Baba, M.; Shigeta, S.; Yuasa, S.; Takashima, H.; Sehiya, K.; Ubasawa, M.; Tanaka, H.; Miyasaka, T.; Walker, R. T.; De Clercq, E. Preclinical evaluation of MKC-442, a highly potent and specific inhibitor of human immunodeficiency virus type 1 in vitro. *Antimicrob. Agents Chemother.* **1994**, *38*, 688−692.

(22) Pauwels, R.; Balzarini, J.; Baba, M.; Snoeck, R.; Schols, D.; Herdewijn, P.; Desmyter, J.; De Clercq, E. Rapid and automated tetrazolium-based colorimetric assay for the detection of anti-HIV compounds. *J. Virol. Methods* **1988**, *20*, 309−321.

(23) Stammers, D. K.; Somers, D. O. N.; Ross, C. K.; Kirby, I.; Ray, P. H.; Wilson, J. E.; Norman, M.; Ren, J. S.; Esnouf, R. M.; Garman, E. F.; Jones, E. Y.; Stuart, D. I. Crystals of HIV-1 reverse transcriptase diffracting to 2.2 Å resolution. *J. Mol. Biol.* **1994**, *242*, 586−588.

(24) Esnouf, R. M.; Ren, J.; Garman, E. F.; Somers, D. O. N.; Ross, C. K.; Jones, E. Y.; Stammers, D. K.; Stuart, D. I. Continuous and discontinuous changes in the unit cell of HIV-1 reverse transcriptase crystals on dehydration. *Acta Crystallogr.* **1998**, *D54*, 938−954.

(25) Otwinowski, Z.; Minor, W. Processing of X-ray diffraction data collected in oscillation mode. *Methods Enzymol.* **1996**, *276*, 307−326.

(26) Brunger, A. T. 1992 *X-PLOR Manual;* Yale University Press: New Haven, CT.

(27) Brunger, A. T.; Adams, P. D.; Clore, G. M.; Delano, W. L.; Gros, P.; Grosse, K. R. W.; Jiang, J. S.; Kuszewski, J.; Nilges, M.; Pannu, N. S.; Read, R. J.; Rice, L. M.; Simonson, T.; Warren, G. L. Crystallography and NMR system: A new software suite for macromolecular structure determination. *Acta Crystallogr.* **1998**, *D54*, 905−921.

(28) Jones, T. A. Interactive computer graphics: FRODO. *Methods Enzymol.* **1985**, *115*, 157−171.

(29) Esnouf, R. M. Further additions to Molscript version 1.4, including reading and contouring of electron-density maps. *Acta Crystallogr.* **1999**, *D55*, 938−940.

(30) Merritt, E. A.; Murphy, M. E. P. Raster3D version 2.0. A program for photorealistic molecular graphics. *Acta Crystallogr.* **1994**, *D50*, 869−873.

JM990192C